

# Pericardial Effusion Detection on Post-Mortem Computed Tomography Images Using Convolutional Neural Networks

Haoyu KONG<sup>a</sup>, Jia RONG<sup>b,1</sup>, Chris BAIN<sup>a</sup>, Xinyu ZHANG<sup>b</sup>, Sarah PARSONS<sup>c,d</sup>,  
Guanliang CHEN<sup>a</sup> and Richard BASSED<sup>c,d</sup>

<sup>a</sup>Department of Human-Centred Computing, Faculty of Information Technology,  
Monash University, Australia

<sup>b</sup>Department of Data Science and AI, Faculty of Information Technology, Monash  
University, Australia

<sup>c</sup>Department of Forensic Medicine, Faculty of Medicine, Nursing and Health Sciences,  
Monash University, Australia

<sup>d</sup>Victorian Institute of Forensic Medicine, Australia

ORCID ID: Haoyu Kong <https://orcid.org/0000-0003-1207-8203>, Jia Rong  
<https://orcid.org/0000-0002-9462-3924>, Chris Bain <https://orcid.org/0000-0002-5281-2364>, Xinyu Zhang <https://orcid.org/0000-0002-6891-7718>, Guanliang Chen  
<https://orcid.org/0000-0002-8236-3133>, Richard Basset <https://orcid.org/0000-0001-5473-055X>

**Abstract.** Pericardial effusion can be a sign of significant underlying disease and, in some cases, may lead to death. Post-mortem computed tomography (PMCT) is a well-established tool to assist death investigation processes in the forensic setting. In practice, the scarcity of well-trained radiologists is a challenge in processing raw whole-body PMCT images for pericardial effusion detection. In this work, we propose a Pericardial Effusion Automatic Detection (PEAD) framework to automatically process raw whole-body PMCT images to filter out the irrelevant images with heart organ absent and focus on pericardial effusion detection. In PEAD, the standard convolutional neural network architectures of VGG and ResNet are carefully modified to fit the specific characteristics of PMCT images. The experimental results prove the effectiveness of the proposed framework and modified models. The modified VGG and ResNet models achieved superior detection accuracy than the standard architecture with reduced processing speed.

**Keywords.** Pericardial effusion detection, post-mortem computed tomography, convolutional neural network

## 1. Introduction

Pericardial and/or heart disease may be accompanied by pericardial effusion (PE), which refers to the increased amount of fluid inside the pericardial cavity [1]. Detection of PE is essential for diagnosis and treatment in the clinical domain. Clinicians generally diagnose PE by analyzing computed tomography (CT) images or echocardiographic

---

<sup>1</sup> Corresponding Author: Jia Rong, email: [jiarong@acm.org](mailto:jiarong@acm.org).

images [1,2], which requires years of training and working experience to derive into an accurate diagnostic decision. In forensic medicine, whole-body PMCT examinations can support forensic pathologists with detailed information for analysis and avoid dissection due to cultural or family reasons [3]. Manual detection of PE with the aid of PMCT began in 2004 [4]. However, this requires an extensive number of highly trained practitioners and large capital investments, thus, becoming a major challenge for most forensic medical facilities.

Deep learning technologies have significantly impacted many fields in the past two decades, especially the medical domain [5]. The Convolutional Neural Networks (CNN) has shown promising achievements in working with medical images to assist clinicians in making diagnostic decisions more efficiently. Inception-v3 and VGG models have been used in identifying PE cases based on echocardiograms [6,7] and positron emission tomography images [8]. Few works [3-9] have been reported in PE detection from forensic images. A limited number of available cases with pixel-level labels and a lack of appropriate sampling selections make the detection task even difficulty. Besides, the classic CNN models, such as VGG and Res Net, require high computational costs in processing a large amount of data, being less efficient. Therefore, we urgently need more effective models to address such challenges.

Accordingly, we propose the “Pericardial Effusion Automatic Detection” (PEAD) framework, which allows forensic personnel to quickly and accurately detect the presence of pericardial effusion. To assist forensic pathologists in workload management, the proposed framework inputs the stack of whole-body PMCT and automatically discards the irrelevant sample slices where cardiac tissues are absent. The remaining cardiac PMCT slices are further analysed for the PE detection. Considering classic CNN models are designed for natural images, we modified two CNN models with simplified structures but kept promising performance.

In summary, this work contributes as follows: (1) introducing a framework that assists pathologists in detecting PE using whole-body PMCT images, and (2) providing two simplified CNNs based on VGG and ResNet architectures to achieve accurate diagnosis with low computational cost.

## 2. Methods

### 2.1. The PEAD framework

Figure 1 demonstrates the proposed PEAD framework. The raw PMCT scans are in 3D DICOM format, which are transformed into grey-scale 2D sample slices extracted every 10 mm and resized to 224×224 pixels. The 10-fold cross-validation method was applied to evaluate the performance of the proposed models.

Stage 1 aims to recognize the heart organ from images to filter out irrelevant samples. Only those with heart presented are kept and taken as the input for Stage 2. Nearly 85% of the processing time can be saved by adopting this filtering operation compared to direct detection on all raw whole-body scans without any manual intervention. Stage 2 checks each remaining sample for PE detection. A series of ablation experiments were conducted to compare the performance of various CNN architectures. The results show that VGG and ResNet models obtained higher classification accuracies (around 85%).

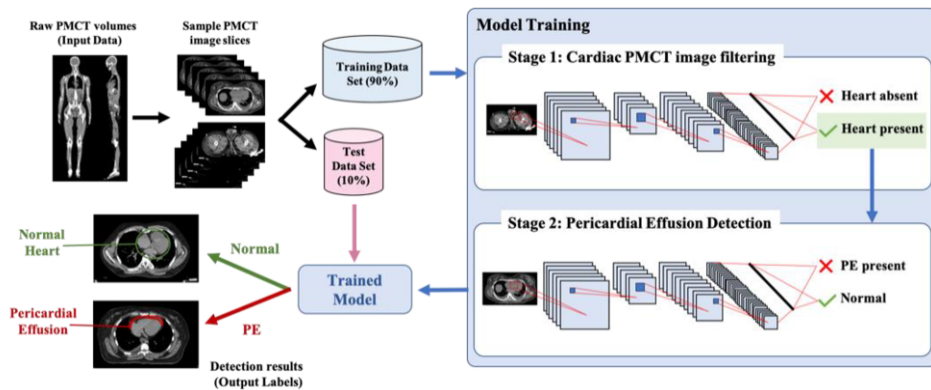


Figure 1. The Pericardial Effusion Automatic Detection (PEAD) framework.

### 2.2. Modified CNN models for PMCT image processing

The standard VGG [9] and ResNet [10] models were designed to classify natural images. With an increased number of layers, the accuracy can be enhanced accordingly, such as ResNet101 [10]. However, such an approach could potentially increase the computational cost. Therefore, a task-specific CNN is generally required to outperform standard models when dealing with small-scale image sets [11]. Besides, PMCT images are naturally simpler in context than natural ones due to the fixed acquisition angle and positions of organs. Accordingly, we reduced the number of layers in the standard VGG and ResNet architectures to keep the minimum complexity of the models. Figure 2 shows the new structures of the modified ResNet10 and VGG8 models.

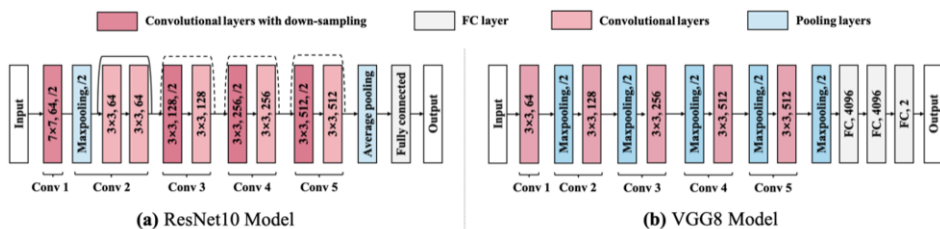


Figure 2. The modified ResNet10 and VGG8 models.

Only five convolution modules (Cov 1 to Cov 5) were kept in both models. In ResNet10, a basic residual block with an identity shortcut was applied to the second convolution module (Cov 2). The remaining three convolution modules adopted special residual basic blocks with a stride of 2 for subsequent feature extraction and down-sampling. Average pooling was used to speed up processing without loss of accuracy [10]. VGG8 has five convolutional layers and three fully connected (FC) layers to produce the probability of the presence of PE as the final output.

The complexity of the models was measured by floating point operations per second (FLOPs) [12], calculated as:

$$FLOPs = (K_h \times K_w \times C_{in} \times C_{out} + C_{out}) \times H \times W \quad (1)$$

where  $K_h$  is the kernel height and  $K_w$  is the kernel width.  $C_{in}$  and  $C_{out}$  are the channel number of input and output,  $H$  and  $W$  refer to the output feature map's height and width.

ResNet10 is expected to be the shortest training and test time with  $8.10 \times 10^8$  FLOPs followed by VGG8 with  $3.39 \times 10^9$ .

### 3. Results

Ninety anonymous deceased individuals from the publicly available New Mexico Decedent Image Database (NMDID) were applied in this work [13], including 45 males ( $\pm 0.4$ ) and 45 females ( $\pm 2.5$ ). 44 of them presented with PE, and 46 had a normal heart. After pre-processing, 2,775 PMCT slices were extracted. 1,502 slices have heart organs, 670 were labelled as PE, and 832 were normal.

A set of experiments were conducted to assess the proposed PEAD framework and the modified models. Eight standard CNN models [9,10]: VGG11, VGG13, VGG16, VGG19, ResNet18, ResNet34, ResNet50 and ResNet101, were involved for comparison. The details are as follows in Table 1.

**Table 1:** Performance comparison between proposed PEAD-based and baseline models in PE detection.

Classifier	Acc.	Prec.	Rec.	FPR	F1	AUC	IPS	#Para.	FLOPs
PEAD-R10-V8	<b>0.8941</b>	0.9392	<b>0.9236</b>	0.2087	<b>0.9313</b>	<b>0.9320</b>	185.66	128.37	5.23
PEAD-V8-V8	0.8933	0.9386	0.9229	0.2087	0.9306	0.9313	140.22	246.92	6.90
PEAD-R10-R10	0.8872	<b>0.9439</b>	0.9106	<b>0.1990</b>	0.9270	0.9206	271.72	<b>9.83</b>	<b>3.50</b>
PEAD-R10-R19	0.8842	0.9316	0.9173	0.2389	0.9244	0.9234	86.26	144.49	21.43
R10	<b>0.8720</b>	0.9555	<b>0.8852</b>	0.1907	<b>0.9190</b>	<b>0.8990</b>	<b>549.69</b>	<b>4.91</b>	<b>1.78</b>
R101	0.8567	0.9625	0.8676	0.1782	0.9126	0.8899	111.89	42.5	15.66
V8	0.8591	0.9363	0.8840	0.2636	0.9094	0.8817	280.35	123.46	3.45
V19	0.8473	<b>0.9689</b>	0.8567	<b>0.1349</b>	0.9094	0.8711	102.32	139.58	19.65

Table 1 summarizes the performance of five PEAD-based models and baseline classifiers for the PE detection task. With simpler structure, the modified model, ResNet10, overperformed all standard models except VGG19 on precision (Prec.) and false positive rate (FPR). The PEAD-based models with two CNNs provide better performance than the baseline models. Particularly, the proposed PEAD-based model with ResNet10 in Stage 1 and VGG8 in Stage 2 (PEAD-R10-V8) achieved the highest F1 scores 93%. A high recall (Rec. /true positive rate, TPR) score indicates all PEAD-based models are sensitive to PE. With the least number of parameters (#Para.) involved, R10 and PEAD-R10-R10 were the fastest models. PEAD-R10-R10 took approximate 94.5 minutes to complete the training and testing on the entire dataset of 2,775 PMCT slices.

### 4. Discussion

The proposed PEAD framework aims to optimize the PE detection process. Experiments show that the framework can improve the sensitivity of the detection process by classifying cardiac PMCT images first and detecting PE based on them. Since the PEAD framework emulates the human detection pipeline, the results produced by the PEAD framework are more interpretable than those produced by the method that directly classifies PE on the whole-body PMCT dataset.

Since this work is the first of its kind which adopts PMCT to detect PE, there is no existing literature to be compared. For fair evaluation, we evaluated 18 models and two modified ones on the same task. The experimental results support our view that the models with fewer convolutional layers can achieve a close result to the standard models in the task of heart and PE classification. Moreover, the simplified models can save storage space while maintaining accuracy. This also makes it possible to deploy CNN-based PE detection algorithms on devices with limited storage space.

## 5. Conclusions

A CNN-based PEAD framework with modified VGG and ResNet (VGG8 and ResNet10) is proposed in this work to improve efficiency for PE detection from whole-body PMCT images automatically. Since real-life PMCT images and labels are not easy to obtain, the data resource is always a limitation of the related work in PE detection. This paper is our initial work, and we aim to obtain more cases for use in future work.

## References

- [1] Pérez-Casares A, Cesar S, Brunet-Garcia L, Sanchez-de Toledo J. Echocardiographic evaluation of pericardial effusion and cardiac tamponade. *Front Pediatr.* 2017 Feb;5:4, doi: [10.3389/fped.2017.00079](https://doi.org/10.3389/fped.2017.00079).
- [2] Pao TH, Chang WL, Chiang NJ, Lin CY, Lai WW, Tseng YL, Lin FC. Pericardial effusion after definitive concurrent chemotherapy and intensity modulated radiotherapy for esophageal cancer. *Radiat Oncol.* 2020 Dec;15:1-10, doi: [10.1186/s13014-020-01498-3](https://doi.org/10.1186/s13014-020-01498-3).
- [3] Ebert LC, Heimer J, Schweitzer W, Sieberth T, Leipner A, Thali M, Ampanozi G. Automatic detection of hemorrhagic pericardial effusion on PMCT using deep learning—a feasibility study. *Forensic Sci Med Pathol.* 2017 Dec;13(4):426-31, doi: [10.1007/s12024-017-9906-1](https://doi.org/10.1007/s12024-017-9906-1).
- [4] Shiotani S, Watanabe K, Kohno M, Ohashi N, Yamazaki K, Nakayama H. Postmortem computed tomographic (PMCT) findings of pericardial effusion due to acute aortic dissection. *Radiat Med.* 2004 Nov;22(6):405-7, doi: [10.1007/s12024-017-9906-1](https://doi.org/10.1007/s12024-017-9906-1).
- [5] Nazir M, Shakil S, Khurshid K. Role of deep learning in brain tumor detection and classification (2015 to 2020): A review. *Comput Med Imaging Graph.* 2021 Jul;91:101940, doi: [10.1016/j.compmedimag.2021.101940](https://doi.org/10.1016/j.compmedimag.2021.101940).
- [6] Madani A, Arnaout R, Mofrad M, Arnaout R. Fast and accurate view classification of echocardiograms using deep learning. *NPJ Digit Med.* 2018 Mar;1(1):1-8, doi: [10.1038/s41746-017-0013-1](https://doi.org/10.1038/s41746-017-0013-1).
- [7] Nayak A, Ouyang D, Ashley EA. A DEEP LEARNING ALGORITHM ACCURATELY DETECTS PERICARDIAL EFFUSION ON ECHOCARDIOGRAPHY. *J Am Coll Cardiol.* 2020 Mar;75(11 Supplement 1):1563, doi: [10.1016/S0735-1097%2820%2932190-2](https://doi.org/10.1016/S0735-1097%2820%2932190-2).
- [8] Zhang J, Zhang Z, Ji X, Ren W, Cheng Y, Wang C, Kan Q. Deep learning convolutional neural network in diagnosis of serous effusion in patients with malignant tumor by tomography. *J Supercomput.* 2022 Feb;78(3):4449-66, doi: [10.1007/s11227-021-04051-5](https://doi.org/10.1007/s11227-021-04051-5).
- [9] Simonyan K, Zisserman A. Very deep convolutional networks for large-scale image recognition. *arXiv preprint arXiv:1409.2014* Sep; 6:1556, doi: [10.48550/arXiv.1409.1556](https://doi.org/10.48550/arXiv.1409.1556).
- [10] He K, Zhang X, Ren S, Sun J. Deep residual learning for image recognition. In *Proceedings of the IEEE conference on computer vision and pattern recognition 2016*;770-8, doi: [10.1109/CVPR.2016.90](https://doi.org/10.1109/CVPR.2016.90).
- [11] Shin HC, Roth HR, Gao M, Lu L, Xu Z, Nogues I, Yao J, Mollura D, Summers RM. Deep convolutional neural networks for computer-aided detection: CNN architectures, dataset characteristics and transfer learning. *IEEE Trans Med Imaging.* 2016 Feb;35(5):1285-98, doi: [10.1109/tmi.2016.2528162](https://doi.org/10.1109/tmi.2016.2528162).
- [12] Molchanov P, Tyree S, Karras T, Aila T, Kautz J. Pruning convolutional neural networks for resource efficient inference. *arXiv preprint arXiv.* 2016 Nov;1611:06440. doi: [10.48550/arXiv.1611.06440](https://doi.org/10.48550/arXiv.1611.06440).
- [13] Edgar H, Daneshvari BS, Moes E, Adolph N, Bridges P, Nolte K. New mexico decedent image database, Office of the Medical Investigator, University of New Mexico: Albuquerque, NM, USA (2020), doi: [10.25827/5s8c-n515](https://doi.org/10.25827/5s8c-n515).